Observational signatures of $f(R)$ dark energy models that satisfy cosmological and local gravity constraints

Shinji Tsujikawa[1]

[1]*Department of Physics, Gunma National College of Technology, Gunma 371-8530, Japan*

(Received 10 September 2007; published 11 January 2008)

We discuss observational consequences of $f(R)$ dark energy scenarios that satisfy local gravity constraints (LGC) as well as conditions of the cosmological viability. The model we study is given by $m(r) = C(-r-1)^p$ $(C > 0,\ p > 1)$ with $m = Rf_{,RR}/f_{,R}$ and $r = -Rf_{,R}/f$, which covers viable $f(R)$ models proposed so far in a high-curvature region designed to be compatible with LGC. The equation of state of dark energy exhibits a divergence at a redshift z_c that can be as close as a few while satisfying sound horizon constraints of the cosmic microwave background (CMB). We study the evolution of matter density perturbations in detail and place constraints on model parameters from the difference of spectral indices of power spectra between CMB and galaxy clustering. The models with $p \geq 5$ can be consistent with those observational constraints as well as LGC. We also discuss the evolution of perturbations in the Ricci scalar R and show that an oscillating mode (scalaron) can easily dominate over a matter-induced mode as we go back to the past. This violates the stability of cosmological solutions, thus posing a problem about how the overproduction of scalarons should be avoided in the early universe.

DOI: 10.1103/PhysRevD.77.023507 PACS numbers: 98.80.−k

I. INTRODUCTION

The origin of dark energy (DE) has persistently been one of the most serious problems in cosmology [1,2]. Many DE models have been proposed so far, but we have not found any strong evidence to support that such models are better than the cosmological constant. Thus the first step towards the understanding of the origin of DE is to find the departure from the ΛCDM model.

The simplest modification to the ΛCDM model is perhaps so-called $f(R)$ gravity in which the Lagrangian is written in terms of the function of a Ricci scalar R. It is well known that inflationary expansion is realized by the Starobinsky model with a Lagrangian density $f(R) = R + \alpha R^2$ [3]. Since the R^2 term is negligibly small relative to R at the present epoch, this model is not suitable to explain present accelerated expansion of the Universe. Instead, the model with a Lagrangian density $f(R) = R - \alpha/R^n$ $(\alpha > 0,\ n > 0)$ was proposed to give rise to a late-time accelerated expansion in the metric formalism [4] (see also Refs. [5,6]). However it was shown that this model is plagued by matter instability [7] as well as by a difficulty to satisfy local gravity constraints [8]. Moreover it does not possess a standard matter-dominated epoch because of a large coupling between dark energy and dark matter [9] (see Refs. [10] for recent works).

In Ref. [11] several conditions for the cosmological viability of $f(R)$ dark energy models were derived without specifying the forms of $f(R)$. This can be well understood by considering a trajectory of each model in the (r, m) plane, where $r \equiv -Rf_{,R}/f$ and $m \equiv Rf_{,RR}/f_{,R}$. The existence of a saddle matter-dominated epoch requires the conditions $m > 0$ and $-1 < \mathrm{d}m/\mathrm{d}r \leq 0$ around the point $(r, m) = (-1, 0)$. The matter era can be followed by a stable de-Sitter attractor on the line $r = -2$ provided that $0 < m(r = -2) \leq 1$. This method is useful to rule out some of the $f(R)$ models such as $f(R) = R - \alpha/R^n$ $(\alpha > 0,\ n > 0)$ easily.

More recently a sequence of cosmologically viable $f(R)$ models was discussed in Refs. [12,13]. One such model, for example, is $f(R) = (R^b - \Lambda)^{1/b}$ with $0 < b < 1$, which corresponds to a straight line $m(r) = (b-1)(r+1)$ connecting the matter point $(r, m) = (-1, 0)$ to the de-Sitter point on the line $r = -2$. The parameter m that characterizes the deviation from the ΛCDM model is constrained to be $m < \mathcal{O}(0.1)$ for such models from the data of Supernova Ia (SN Ia) and cosmic microwave background (CMB) [13]. Meanwhile local gravity experiments constrain the value of m to be very much smaller than unity in high-density regions where gravity experiments are carried out. This means that the deviation from the ΛCDM model needs to be very small in a high-curvature cosmological epoch whose Ricci scalar R is much larger than the present cosmological value R_0.

A number of authors [14–16] recently proposed $f(R)$ dark energy models that can satisfy both cosmological and local gravity constraints (LGC) (see Refs. [17,18] for related works). From the requirement of LGC these behave as close as the ΛCDM model during radiation and matter-dominated epochs $(R \gg R_0)$. The deviation from the ΛCDM model becomes significant after the end of the matter era with the growth of the quantity m. These models satisfy the relation $f(R = 0) = 0$, implying that the cosmological constant disappears in a flat spacetime. We note, however, that the Ricci scalar is frozen at a value $R = R_1 > 0$ if the solutions are trapped by stable de-Sitter attractors responsible for the late-time acceleration. Thus, in these models the system does not reach the region $R = 0$ in an asymptotic future.

 © 2008 The American Physical Society

In this paper we shall study observational consequences of $f(R)$ models that satisfy LGC in addition to conditions of cosmological viability. The models we consider are given by $m(r) = C(-r-1)^p$ with $C > 0$ and $p > 1$, which cover viable models proposed in the literature [14–16] in the region $R \gg R_0$. The quantity $m(r)$ is, for large p, vanishingly small during matter and radiation epochs ($r \approx -1$), but grows to the order of C as the solutions approach de-Sitter attractors on the line $r = -2$. These models exhibit peculiar evolution of the DE equation of state, as we will see later. Moreover matter density perturbations evolve differently compared to the ΛCDM cosmology for redshifts below a critical value z_k. This property can be used to place constraints on model parameters in addition to constraints coming from LGC, SN Ia, and CMB.

This paper is organized as follows. In Sec. II we present all conditions viable $f(R)$ DE models need to satisfy. In addition to $f(R)$ models studied so far, we shall propose another model satisfying these conditions. In Sec. III the evolution of the DE equation of state and the resulting observational consequences are discussed in addition to constraints coming from the sound horizon of CMB. In Sec. IV we study how matter perturbations evolve on subhorizon scales and put constraints on model parameters from the difference of spectral indices of the power spectra between CMB and galaxy clustering. We also discuss the evolution of the perturbation δR and show that an oscillating mode called scalaron [3] easily dominates over the background value R when we go back to the past. This generally violates the stability condition of $f(R)$ models, which gives rise to another problem about how to avoid the overproduction of scalarons in the early universe. We conclude in Sec. V.

II. MODELS THAT SATISFY COSMOLOGICAL AND LOCAL GRAVITY CONSTRAINTS

Let us begin with the following action

$$S = \int d^4x\sqrt{-g}\left[\frac{1}{2\kappa^2}f(R) + \mathcal{L}_{\rm m} + \mathcal{L}_{\rm rad}\right], \qquad (1)$$

where $\kappa^2 = 8\pi G$ (G is a bare gravitational constant). In what follows we use the unit $\kappa^2 = 1$, but we restore the gravitational constant when it is needed. Note that $\mathcal{L}_{\rm m}$ and $\mathcal{L}_{\rm rad}$ are the Lagrangian densities of dustlike matter and radiation, respectively, which satisfy usual conservation equations. In the flat Friedmann-Robertson-Walker (FRW) background with a scale factor a, the Ricci scalar is given by $R = 6(2H^2 + \dot{H})$, where $H \equiv \dot{a}/a$ is a Hubble parameter and a dot represents a derivative with respect to cosmic time t.

There are a number of constraints viable $f(R)$ models need to satisfy. First of all, to avoid antigravity, we require the condition $f_{,R} \equiv df/dR > 0$. Modified $f(R)$ models possess a scalar particle whose effective mass is given by

$$M^2(R) \simeq \frac{1}{3f_{,RR}}, \qquad (2)$$

in the regime $M^2(R) \gg R$ [13,15,17,19]. In order to avoid that the scalaron becomes tachyons or ghosts, we require $f_{,RR} \equiv {\rm d}^2f/{\rm d}R^2 > 0$ in this region. Note that this condition can be also derived by considering the stability of perturbations [19,20].

The conditions for the cosmological viability of $f(R)$ models have been studied in Ref. [11] in great detail. This can be well understood by considering two quantities:

$$m = \frac{Rf_{,RR}}{f_{,R}}, \qquad r = -\frac{Rf_{,R}}{f}. \qquad (3)$$

The ΛCDM model, $f(R) = R - 2\Lambda$, corresponds to $m = 0$ and $r = -R/(R-2\Lambda)$. The quantity m characterizes the deviation from the ΛCDM model. The cosmological viability of such models is known by plotting corresponding curves in the (r, m) plane.

In what follows we shall consider cosmological evolution that starts from a radiation epoch with large and positive R followed by a matter era and eventually approaches a de-Sitter attractor with $R = R_1 > 0$ in future.[1] In cosmologically viable models we study, the quantity m is always smaller than 1 with $f_{,R}$ of order unity before reaching a de-Sitter attractor. Since $1/f_{,RR} \gg R$ in such cases, one can use the scalaron mass given in Eq. (2). Hence the stability conditions are given by [15]

$$f_{,R} > 0, \qquad f_{,RR} > 0, \quad \text{for } R \geq R_1. \qquad (4)$$

The matter-dominated point P_M exists on the line $m = -r - 1$ with m close to 0, i.e., $(r, m) \approx (-1, 0)$. The presence of a viable saddle matter era demands the conditions [11] (see also Ref. [21]):

$$m(r \approx -1) > 0, \quad \text{and} \quad -1 < \frac{{\rm d}m}{{\rm d}r}(r \approx -1) \leq 0. \qquad (5)$$

If the condition (4) is satisfied then the variable m is automatically positive. The second requirement in Eq. (5) implies that $m(r)$ curves should be present between the lines $m = 0$ and $m = -r - 1$.

There is a stable de-Sitter fixed point that leads to a late-time acceleration:

$$P_A\colon\ r = -2, \qquad 0 < m \leq 1. \qquad (6)$$

If a $m(r)$ curve staring from P_M has an intersection point with a line $r = -2$ in the region $0 < m \leq 1$, the corresponding $f(R)$ model is regarded as cosmologically viable. The ΛCDM model is a straight line that links P_M: $(r, m) = (-1, 0)$ with P_A: $(r, m) = (-2, 0)$. In this paper we do not consider another accelerated fixed point P_B that exists on the line $m = -r - 1$ with $(\sqrt{3} - 1)/2 < m \leq 1$ [11]. This

[1] During the radiation era the Ricci scalar evolves as $R \propto t^{-3/2}$ because of the presence of nonrelativistic particles.

corresponds to the case in which R continues to decrease in future, which can violate the stability condition (4).

A number of $f(R)$ models satisfying the above conditions were considered in Refs. [12,13]. Some examples are

$$\text{(i) } f(R) = (R^b - \Lambda)^c \qquad (c \geq 1, bc \approx 1), \tag{7}$$

$$\text{(ii) } f(R) = R - \alpha R^n \qquad (\alpha > 0, 0 < n < 1), \tag{8}$$

which correspond to $m(r) = [(1-c)/c]r + b - 1$ and $m(r) = n(1+r)/r$, respectively.

Let us next consider local gravity constraints on $f(R)$ dark energy models. The LGC are satisfied for $M\ell \gg 1$ [13,17], where ℓ is a scale at which gravity experiments are carried out. Using Eqs. (2) and (3), this constraint is expressed by

$$m(R_s) \ll \frac{1}{f_{,R_s}} \left(\frac{\ell}{R_s^{-1/2}} \right)^2, \tag{9}$$

where R_s is a curvature measured on the local structure and is proportional to the energy density ρ_s of the structure ($R_s \approx 8\pi G \rho_s$). Using the present cosmological density ρ_0 and the Hubble radius $H_0^{-1} \sim 10^{28}$ cm (in what follows we use the subscript "0" for present values), the above constraint is rewritten as

$$m(R_s) \ll \frac{\rho_s}{\rho_0} \left(\frac{\ell}{H_0^{-1}} \right)^2, \tag{10}$$

where we used $f_{,R_s} \sim 1$ and $R_0 \sim H_0^2 \sim 8\pi G \rho_0$. The r.h.s. of Eq. (10) is very much smaller than unity [13] because $\ell \ll H_0^{-1}$ even though ρ_s is larger than ρ_0. In the case of the Cavendish-type experiments the typical constraint is $m(R_s) \ll 10^{-43}$, as we will see later. Note that under the so-called chameleon approach [22] the parameter $m(R_s)$ is also constrained to be very much smaller than unity [23].

The above argument shows that in the high-curvature region ($R \gg R_0$) the quantity m needs to be negligibly small. Cosmologically this means that during radiation and matter eras the models need to mimic the ΛCDM model with a high precision. Note that the models (i) and (ii) given in Eqs. (7) and (8) behave as $m(r) = C(-r-1)$ as r approaches -1. In such cases, however, LGC are difficult to be satisfied unless C is chosen to be unnaturally small.

Hu and Sawicki [14] proposed an explicit $f(R)$ model that satisfies both cosmological and local gravity constraints. It is given by

$$f(R) = R - \lambda R_c \frac{(R/R_c)^{2n}}{(R/R_c)^{2n} + 1}, \tag{11}$$

where the power $2n$ is used instead of n. Starobinsky [15] also proposed another viable model:

$$f(R) = R - \lambda R_c \left[1 - \left(1 + \frac{R^2}{R_c^2} \right)^{-n} \right]. \tag{12}$$

In both models n, λ, and R_c are positive constants, where R_c is the order of the present Ricci scalar R_0. Since $f(R = 0) = 0$ cosmological constant disappears in a flat spacetime. Thus the origin of dark energy can be regarded as the geometrical one.

Let us check the cosmological viability as well as the stability for such models. In the region $R \gg R_c$ these behave as

$$f(R) \simeq R - \lambda R_c \left[1 - \left(\frac{R_c}{R} \right)^{2n} \right], \tag{13}$$

$$r \simeq -1 - \lambda \frac{R_c}{R}, \tag{14}$$

$$m \simeq \frac{2n(2n+1)}{\lambda^{2n}} (-r-1)^{2n+1}. \tag{15}$$

Thus in this region the models (11) and (12) have the following property

$$m(r) = C(-r-1)^p, \tag{16}$$

where $p = 2n + 1 > 1$ and C is a positive constant. It is obvious that, for larger p, $m(r)$ becomes very small as $r \to -1$ so that the model satisfies LGC. Since $\frac{dm}{dr}(r = -1) = 0$ the condition (5) is also satisfied.

Let us next check the conditions (4) and (6). In the model (11), the de-Sitter point at $r = -2$ is determined by the value of λ:

$$\lambda = \frac{(1 + x_1^{2n})^2}{x_1^{2n-1}(2 + 2x_1^{2n} - 2n)}, \tag{17}$$

where $x_1 = R_1/R_c$. From the stability condition $0 < m(r = -2) \leq 1$ we obtain

$$2x_1^{4n} - (2n-1)(2n+4)x_1^{2n} + (2n-1)(2n-2) \geq 0. \tag{18}$$

When $n = 1$, for example, we have $x_1 \geq \sqrt{3}$ and $\lambda \geq 8\sqrt{3}/9$. Under Eq. (18) one can show that the condition (4) is satisfied. This situation is similar to the Starobinsky model (12), see Ref. [15] for details.

We can extend the above two models to the more general form

$$f(R) = R - \xi(R), \qquad \xi(0) = 0, \qquad \xi(R \gg R_c) \to \text{const.} \tag{19}$$

The conditions (4) translate into

$$\xi_{,R} < 1, \qquad \xi_{,RR} < 0, \quad \text{for } R \geq R_1. \tag{20}$$

In order to satisfy LGC, we require that $\xi(R)$ approaches a constant rapidly as R grows in the region $R \gg R_c$ (such as $\xi(R) \simeq \text{const.} - (R_c/R)^{2n}$ discussed above). Another model to meet these requirements is

$$f(R) = R - \lambda R_c \tanh\left(\frac{R}{R_c}\right), \tag{21}$$

where λ and R_c are positive constants. A similar model was proposed by Appleby and Battye [16], although it is different from (21) in the sense that $\xi(R)$ can be negative for $R < R_1$. In the region $R \gg R_c$ the model (21) behaves as $f(R) \simeq R - \lambda R_c[1 - \exp(-2R/R_c)]$, which can be regarded as the special case of (16) with a limit $p \to \infty$. The Ricci scalar at the de-Sitter point is determined by λ, as

$$\lambda = \frac{x_1 \cosh^2(x_1)}{2\sinh(x_1)\cosh(x_1) - x_1}, \tag{22}$$

where $x_1 = R_1/R_c$. From the stability condition (6) of the de-Sitter point we obtain the constraint

$$x_1 > 0.920, \qquad \lambda > 0.905. \tag{23}$$

In the models (11) and (12), $f_{,RR}$ are negative for $0 < R/R_c < [(2n-1)/(2n+1)]^{1/2n}$ and $0 < R/R_c < 1/\sqrt{2n+1}$, respectively. In the model (11) the quantity $f_{,R}$ also becomes negative (i.e., $\xi_{,R} > 1$) in some regions, whereas in the model (12) it is possible to have $f_{,R} > 0$ for all positive R in some restricted regions of the parameter space ($0.944 < \lambda < 0.966$ for $n = 2$). See the curves (i) and (ii) in Fig. 1 for illustration. Of course we are considering the situation in which the violation of the conditions $f_{,R} > 0$ and $f_{,RR} > 0$ occurs for $R < R_1$, so it is harmless as long as the universe is in the region $R \geq R_1$. In the model (21) we always have $f_{,RR} > 0$ for positive R, whereas $f_{,R}$ is positive for $\lambda < 1$. Hence, if $0.905 < \lambda < 1$, this model satisfies the conditions $f_{,R} > 0$ and $f_{,RR} > 0$ for all positive R and also possesses a de-Sitter attractor. Such an example is plotted as the case (iii) in Fig. 1.

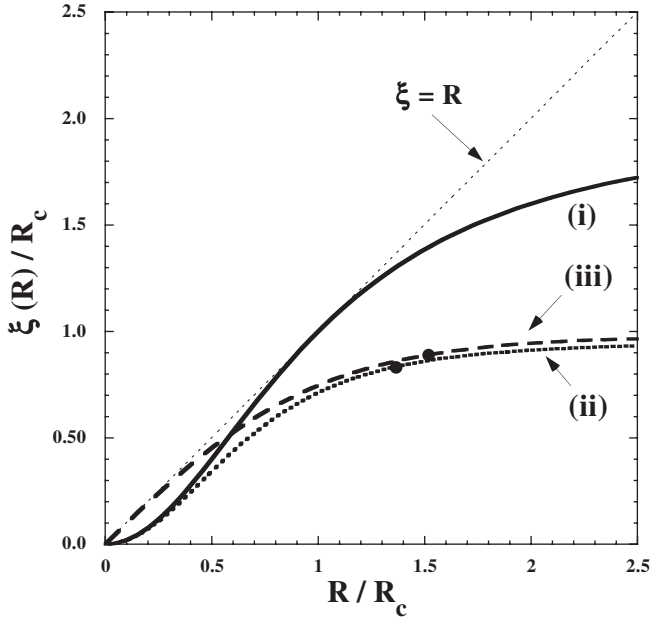

FIG. 1. The illustration of $\xi(R)$ as a function of R/R_c in three different models. Each corresponds to (i) the model (11) by Hu and Sawicki with $n = 1$ and $\lambda = 2$, (ii) the model (12) by Starobinsky with $n = 2$ and $\lambda = 0.95$, and (iii) the model (21) with $\lambda = 0.98$. We also plot a line $\xi(R) = R$ to see whether or not the condition $\xi_{,R} < 1$ (i.e., $f_{,R} > 0$) is violated. The black points represent de-Sitter fixed points ($R = R_1$). Note that in the case (i) the de-Sitter point corresponds to $R_1/R_c = 3.383$, which is outside of the figure. In the case (i) we have $f_{,R} < 0$ for $0.296 < R/R_c < 1$, whereas in the cases (ii) and (iii) $f_{,R} > 0$ for all positive R. In the models (11) and (12) it is inevitable to avoid that $f_{,RR}$ becomes negative in the small R region, but in the model (21) it is possible to realize $f_{,RR} > 0$ for $R > 0$. In the region before the solutions reach the de-Sitter attractor (i.e., $R \geq R_1$), both $f_{,R}$ and $f_{,RR}$ are positive in the above three models.

In Fig. 2 we plot the trajectories in the (r, m) plane for the model (12) with $n = 2$, $\lambda = 0.95$, and for the model (21) with $\lambda = 0.95$. The solutions start from the region $R/R_c \gg 1$ around the point P_M and they finally approach the de-Sitter point P_A at $R = R_1$. Since $f_{,R} > 0$ ($R > 0$) and $f(0) = 0$ in such cases we have $f(R) > 0$ for positive R, which means that $r = -Rf_{,R}/f$ is always negative. The quantity $m = Rf_{,RR}/f_{,R}$ is positive for $R \geq R_1$ because $f_{,RR} > 0$. In the case (A) of Fig. 2 we have $m < 0$ for $0 < R/R_c < 1/\sqrt{2n+1}$ because $f_{,RR}$ changes the sign. Meanwhile, in the case (B), m is always positive for $R >$

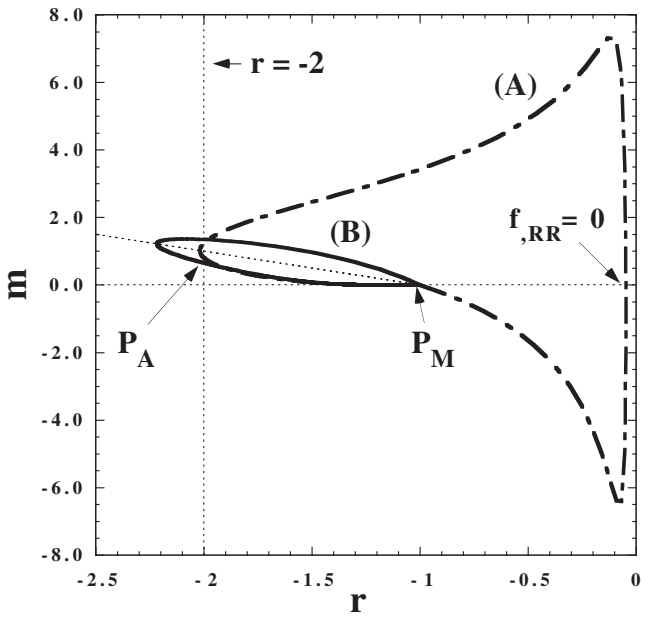

FIG. 2. Two trajectories in the (r, m) plane. The trajectory (A) corresponds to the model (12) by Starobinsky with $n = 2$ and $\lambda = 0.95$, whereas the trajectory (B) to the model (21) $\lambda = 0.95$. In both cases the solutions start from the region around the point P_M: $(r, m) = (-1, 0)$ with $R \gg R_c$. They approach the stable de-Sitter point P_A on the line $r = -2$ with $0 < m \leq 1$. In the case (A) the quantity $f_{,RR}$ becomes negative for $0 < R/R_c < 1/\sqrt{2n+1}$, while $f_{,R}$ is positive for $R > 0$. In the case (B) one has $f_{,RR} > 0$ and $f_{,R} > 0$ for all positive R. In the limit $R/R_c \to 0$ both models approach the point $(r, m) = (-1, 0)$ again.

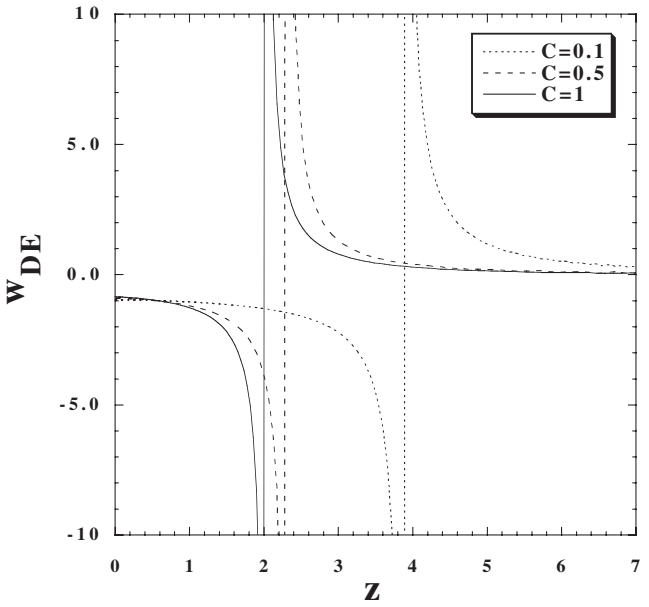

FIG. 3. The DE equation of state $w_{\rm DE}$ versus the redshift z for the model $m(r) = C(-r-1)^2$ with three different parameters ($C = 0.1, 0.5, 1.0$). With the increase of C the divergence of $w_{\rm DE}$ occurs for smaller z.

0. In the limit $R/R_c \to 0$ the trajectories approach the point $(r, m) = (-1, 0)$ again in both models. If the Ricci scalar oscillates around $R = 0$, the quantity $f_{,RR}$ becomes negative for $R < 0$ even for the model (21). As we will see later in detail, this can indeed occur by the oscillation of scalarons unless initial conditions are appropriately chosen. The above argument shows the importance of confining the Ricci scalar in the region $R \geq R_1$ to ensure the stability of models.

In this paper we shall study a number of cosmological constraints on the models of the type (16). As we mentioned, in the region $R \gg R_c$, this covers the models (11) and (12) with $p = 2n + 1$ as well as the model (21) with the limit $p \to \infty$. If $0 < C \leq 1$ there exists a stable de-Sitter point P_A at $r = -2$. The model $m(r) = C(-r-1)^p$ essentially contains sufficient information about how viable $f(R)$ models behave. During radiation and matter eras ($r \simeq -1$) the quantity m is very much smaller than unity, but it grows to the order of C once the system approaches the de-Sitter attractor P_A. Thus one can see the departure from the ΛCDM model around the present epoch. Note that we are only concerned with the region of $m(r)$ curves before the solutions reach the de-Sitter attractor. If we demand the condition $f(R = 0) = 0$, this can be satisfied by modifying the form of $m(r)$ outside the region that connects P_M to P_A [as in the models (12) and (21) in Fig. 2].

Before entering the details of various cosmological constraints, we consider LGC on the model (16). In high-dense regions where local gravity experiments are carried out ($R_s \gg R_c \sim R_0$) the quantity r behaves as Eq. (14) and hence $m \simeq \tilde{m}(R_0/R_s)^p$, where $\tilde{m}$ is a constant whose order is not much different from unity. Since $R_0/R_s \sim \rho_0/\rho_s$, the constraint (10) yields

$$\left(\frac{\rho_s}{\rho_0}\right)^{p+1} \gg \tilde{m}\left(\frac{H_0^{-1}}{\ell}\right)^2. \tag{24}$$

In the Cavendish-type experiments the typical values are $\rho_s \sim 10^{-12}$ g/cm^3 and $\ell \sim 10^{-2}$ cm [24]. Recalling the values $\rho_0 \sim 10^{-29}$ g/cm^3 and $H_0^{-1} \sim 10^{28}$ cm, we find that the LGC is well satisfied for $p \geq 3$.

In the case of solar-system experiments, if we take the typical solar-system length scale $\ell = 1$ Au $= 1.5 \times 10^{13}$ cm with the density $\rho_s \sim 10^{-24}$ g/cm^3 at the distance from Sun [14], we obtain the constraint $p \geq 5$. Meanwhile the so-called Shapiro time-delay effect [25] comes mainly from the gravity contribution around the radius of Sun ($\ell \sim 7.0 \times 10^{10}$ cm) with the density $\rho_s \sim 10^{-15}$ g/cm^3, which gives a much weaker constraint: $p \geq 2$. Thus the constraint $p \geq 5$ is certainly enough to satisfy LGC and is even too tight in some of gravity experiments.

III. SN IA AND CMB SOUND HORIZON CONSTRAINTS

In this section we discuss the cosmological evolution of the model (16) at the background level and confront it with constraints coming from SN Ia and the sound horizon of the CMB. In the flat FRW spacetime the variation of the action (1) leads to the following equations

$$3FH^2 = \rho_{\rm m} + \rho_{\rm rad} + (FR - f)/2 - 3H\dot{F}, \tag{25}$$

$$-2F\dot{H} = \rho_{\rm m} + (4/3)\rho_{\rm rad} + \ddot{F} - H\dot{F}, \tag{26}$$

where $F \equiv \partial f/\partial R$. Here $\rho_{\rm m}$ and $\rho_{\rm rad}$ are the energy densities of a nonrelativistic matter and radiation, respectively, which satisfy the usual conservation equations.

Following Refs. [11,13] we introduce the dimensionless variables

$$x_1 = -\frac{\dot{F}}{HF}, \qquad x_2 = -\frac{f}{6FH^2}, \qquad x_3 = \frac{R}{6H^2}, \qquad x_4 = \frac{\rho_{\rm rad}}{3FH^2}. \tag{27}$$

Then we obtain the dynamical equations [11]

$$x_1' = -1 - x_3 - 3x_2 + x_1^2 - x_1x_3 + x_4, \tag{28}$$

$$x_2' = \frac{x_1x_3}{m} - x_2(2x_3 - 4 - x_1), \tag{29}$$

$$x_3' = -\frac{x_1x_3}{m} - 2x_3(x_3 - 2), \tag{30}$$

$$x_4' = -2x_3x_4 + x_1x_4, \tag{31}$$

where a prime represents a derivative with respect to $N = \ln a$. Since m is a function of $r = x_3/x_2$, the above system is

closed. The energy density and the pressure of DE to confront with SN Ia observations are given in Ref. [13] and the corresponding equation of state (EOS) of DE is

$$w_{\rm DE} = -\frac{1}{3}\frac{2x_3 - 1 + (F/F_0)x_4}{1 - (F/F_0)(1 - x_1 - x_2 - x_3 - x_4)}, \quad (32)$$

where F_0 is the present value.

Our model (16) needs to satisfy the condition $F_{,R} > 0$ for $R \geq R_1$, which leads to the increase of F toward the past as R gets larger. The denominator in Eq. (32) is written as $1 - (F/F_0)\Omega_{\rm m}$, where

$$\Omega_{\rm m} \equiv \frac{\rho_m}{3FH^2} = 1 - x_1 - x_2 - x_3 - x_4. \quad (33)$$

Since $\Omega_{\rm m}$ increases from present to the matter-dominated epoch, it happens that $w_{\rm DE}$ exhibits a divergence at a redshift z_c satisfying $\Omega_{\rm m} = F_0/F$. This is in fact generic to cosmologically viable models that fulfill the criterion (4). The EOS of DE crosses a cosmological constant boundary ($w_{\rm DE} = -1$) at a redshift z_b smaller than z_c [13].

In Fig. 3 we plot $w_{\rm DE}$ versus the redshift $z \equiv a_0/a - 1$ for the model $m(r) = C(-r-1)^2$ with three different values of C. In all simulations the present epoch ($z = 0$) is identified as a matter energy fraction $\Omega_{\rm m} = 0.28$ with a radiation contribution $\Omega_{\rm rad} \equiv \rho_{\rm rad}/3FH^2 \sim 10^{-4}$. Note that the current universe is in the middle of approaching the de-Sitter attractor P_A: $(x_1, x_2, x_3) = (0, -1, 2)$ from the matter point P_M: $(x_1, x_2, x_3) \approx (0, -1/2, 1/2)$. As we see in Fig. 3, $w_{\rm DE}$ is larger than -1 at $z = 0$ and decreases to $-\infty$ as $z \to z_c - 0$ after crossing the cosmological constant boundary at $z = z_b$. For smaller C, z_c gets larger. When $C = 1$ we have $z_c = 2.03$ and $w_{\rm DE}(z = 0) = -0.853$, whereas if $C = 0.5$ we get $z_c = 2.31$ with $w_{\rm DE}(z = 0) = -0.904$. This peculiar behavior of the EOS of DE is an interesting signature to discriminate $f(R)$ models from the ΛCDM cosmology. In particular, the larger deviation from the ΛCDM model leads to a smaller critical redshift z_c that can be reached in future observations.

For the values of p greater than 2, z_c gets larger and $w_{\rm DE}(z = 0)$ tends to be closer to -1. In Table I we show z_b, z_c, and $w_{\rm DE}(z = 0)$ together with present values of m for several different choices of p and C. When $p \geq 5$, if we look at the low redshift region only, the models are hardly distinguishable from the ΛCDM model. Still the EOS of DE shows a peculiar behavior in the high redshift region: $z > 3$. For larger p the cosmological constant boundary crossing occurs at the redshift close to the present epoch. We note that the recent SN Ia data analysis finds some evidence for such a crossing [26]. If future high-precision observations favor models whose EOS corresponds to a phantom ($w_{\rm DE} < -1$) in most of the past epochs relevant to SN Ia observations, this can be the signal of $f(R)$ gravity.

If we use the criterion $w_{\rm DE}(z = 0) < -0.7$ according to the current SN Ia data [27], we find from Table I that the models with $p \geq 2$ satisfy this requirement even when C is as close as unity. The slopes of the EOS, $|dw_{\rm DE}/dz|$, are found to be smaller than the order of 0.1 around the present epoch, which do not provide additional information to constrain models. When $C = 1$, we have $w_{\rm DE}(z = 0) > -0.7$ only for $p \leq 1.4$. Thus the current SN Ia observations do not provide a better constraint on the power p than the one obtained by LGC. It will be interesting, however, to carry out a likelihood analysis using the future data of SN Ia along the line of Refs. [28].

TABLE I. The values z_b, z_c, $w_{\rm DE}(z = 0)$ and $m(z = 0)$ in the model $m(r) = C(-r-1)^p$ for several different choices of p and C.

p	C	z_b	z_c	$w_{\rm DE}(z = 0)$	$m(z = 0)$
1.5	0.1	0.79	3.44	−0.959	0.075
1.5	0.5	0.73	2.24	−0.851	0.244
1.5	1	0.85	2.14	−0.743	0.293
2	0.1	0.62	3.88	−0.969	0.067
2	0.5	0.54	2.31	−0.904	0.220
2	1	0.56	2.03	−0.853	0.285
3	0.1	0.40	5.00	−0.982	0.055
3	0.5	0.33	2.83	−0.955	0.180
3	1	0.32	2.31	−0.936	0.248
5	0.1	0.16	7.25	−0.994	0.037
5	0.5	0.10	4.30	−0.990	0.124
5	1	0.09	3.53	−0.988	0.180

Let us also consider the sound horizon constraint coming from the CMB. The angular size of the sound horizon is defined by

$$\Theta_s = \int_{z_{\rm dec}}^{\infty} \frac{c_s(z)dz}{H(z)} \Big/ \int_0^{z_{\rm dec}} \frac{dz}{H(z)}, \quad (34)$$

where $c_s^2(z) = 1/[3(1 + 3\rho_b/4\rho_\gamma)]$ is the adiabatic baryon-photon sound speed and $z_{\rm dec} \simeq 1089$. From the position of CMB acoustic peaks we obtain the constraint $\Theta_s = 0.5946 \pm 0.0021$ deg from the WMAP 3-year data [29]. For the models in which the effect of dark energy is not negligible during the matter-dominated epoch, the quantity Θ_s is rather strongly modified (as in the coupled quintessence [30]).

In $f(R)$ gravity, if the quantity m is not much smaller than 1 during the matter era, this leads to a considerable change of Θ_s compared to the ΛCDM model. In fact, this happens for the models (7) and (8), as was shown in Ref. [13]. In our model (16) the quantity m is very much smaller than unity during the matter era from the requirement to satisfy LGC. Hence it is easier to satisfy the sound horizon constraint compared to the models (7) and (8). In fact, we have evaluated Θ_s numerically and confirmed that the models with $p \geq 2$ are consistent with the WMAP 3-year data. Thus the data coming from the CMB sound horizon does not provide tighter constraints relative to the SN Ia data.

IV. MATTER PERTURBATIONS AND SCALARON OSCILLATIONS

In this section we study constraints on the model (16) coming from matter density perturbations. Let us consider scalar metric perturbations α, β, φ, and γ about the flat FRW background [31]:

$$ds^2 = -(1+2\alpha)dt^2 - 2a\beta_{,i}dtdx^i + a^2[(1+2\varphi)\delta_{ij} + 2\gamma_{|ij}]dx^i dx^j. \quad (35)$$

In what follows we neglect the contribution of radiation as it is unimportant to discuss the evolution of matter perturbations during the matter-dominated epoch. The energy-momentum tensors of a pressureless matter is decomposed by

$$T^0_0 = -(\rho_m + \delta\rho_m), \qquad T^0_i = -\rho_m v_{m,i}, \quad (36)$$

where v_m is a velocity potential.

Introducing a covariant velocity perturbation, $v \equiv a v_m$, we obtain the following equations of motion in the Fourier space [32] (see also Refs. [20,33]):

$$\alpha = \dot{v}, \quad (37)$$

$$(\delta\rho_m/\rho_m)^{\cdot} = \kappa - 3H\alpha - \frac{k^2}{a^2}v, \quad (38)$$

$$\dot{\kappa} + 2H\kappa + \left(3\dot{H} - \frac{k^2}{a^2}\right)\alpha = \frac{1}{2F}\left[\left(-6H^2 + \frac{k^2}{a^2}\right)\delta F + 3H\delta\dot{F} + 3\delta\ddot{F} - \dot{F}\kappa - 3(2\ddot{F} + H\dot{F})\alpha - 3\dot{F}\dot{\alpha} + \delta\rho_m\right], \quad (39)$$

$$\delta\ddot{F} + 3H\delta\dot{F} + \left(\frac{k^2}{a^2} - \frac{R}{3}\right)\delta F = \frac{1}{3}\delta\rho_m + \dot{F}(\kappa + \dot{\alpha}) + (2\ddot{F} + 3H\dot{F})\alpha - \frac{1}{3}F\delta R, \quad (40)$$

$$-\frac{k^2}{a^2}\varphi + 3H(H\alpha - \dot{\varphi}) + \frac{k^2}{a^2}H\chi = \frac{1}{2F}\left[3H\delta\dot{F} - \left(3\dot{H} + 3H^2 - \frac{k^2}{a^2}\right)\delta F - 3H\dot{F}\alpha - \dot{F}\kappa - \delta\rho_m\right], \quad (41)$$

$$\dot{\chi} + H\chi - \alpha - \varphi = \frac{1}{F}(\delta F - \dot{F}\chi), \quad (42)$$

where k is a comoving wave number and $\kappa \equiv 3(H\alpha - \dot{\varphi}) + (\beta + a\dot{\gamma})k^2/a$. We define a gauge-invariant quantity: $\delta_m \equiv \delta\rho_m/\rho_m + 3Hv$. In the comoving gauge where $v = 0$, we find from Eqs. (37) and (38) that $\alpha = 0$ and $\kappa = \dot{\delta}_m$. Then from Eqs. (39) and (40) we obtain

$$\ddot{\delta}_m + \left(2H + \frac{\dot{F}}{2F}\right)\dot{\delta}_m - \frac{\rho_m}{2F}\delta_m = \frac{1}{2F}\left[\left(-6H^2 + \frac{k^2}{a^2}\right)\delta F + 3H\delta\dot{F} + 3\delta\ddot{F}\right], \quad (43)$$

$$\delta\ddot{F} + 3H\delta\dot{F} + \left(\frac{k^2}{a^2} + \frac{F}{3F_{,R}} - 4H^2 - 2\dot{H}\right)\delta F = \frac{1}{3}\delta\rho_m + \dot{F}\dot{\delta}_m. \quad (44)$$

In the model (16) the quantity $m = Rf_{,RR}/F$ is very much smaller than unity during the matter era with $F \simeq 1$. Since $1/f_{,RR} \gg R$ in such a case, the scalaron mass squared is given by Eq. (2) and satisfies the relation $M^2 \gg R \sim H^2$. In what follows we shall discuss two cases: (A) $M^2 \gg k^2/a^2$ and (B) $M^2 \ll k^2/a^2$, separately. As we will see below, the modes that are initially in the region (A) can enter the region (B) during the matter-dominated epoch.

A. The region $M^2 \gg k^2/a^2$

When $M^2 \gg k^2/a^2$, Eq. (44) is approximately given by

$$\delta\ddot{F} + 3H\delta\dot{F} + M^2\delta F \simeq \tfrac{1}{3}\delta\rho_m, \quad (45)$$

where we used the fact that the variation of the quantity F is negligibly small during the matter era. This is a very good approximation for the model (16), since m is vanishingly small during the matter era.

The general solutions for Eq. (45) are given by the sum of the oscillating solution $\delta F_{\rm osc}$ obtained by setting $\delta\rho_m = 0$ and the special solution $\delta F_{\rm ind}$ of Eq. (45) induced by the presence of matter perturbations $\delta\rho_m$. The former was obtained by Starobinsky [15] for the model (12) in the unperturbed flat FRW background (i.e., $k = 0$). The oscillating part $\delta F_{\rm osc}$ satisfies the equation $(a^{3/2}\delta F_{\rm osc})^{\cdot\cdot} + M^2(a^{3/2}\delta F_{\rm osc}) \simeq 0$. By using the WKB approximation, we obtain the solution

$$\delta F_{\rm osc} \propto a^{-3/2} f_{,RR}^{1/4} \cos\left(\int \frac{1}{\sqrt{3f_{,RR}}}dt\right). \quad (46)$$

During the matter era in which the background Ricci scalar evolves as $R^{(0)} = 4/(3t^2)$, the quantity $f_{,RR}$ has a dependence $f_{,RR} \propto R^{-(p+1)} \propto t^{2(p+1)}$. Hence the evolution of the perturbation, $\delta R_{\rm osc} = \delta F_{\rm osc}/f_{,RR}$, is given by

$$\delta R_{\rm osc} \simeq c t^{-(3p+5)/2}\cos(c_0 t^{-p}), \quad (47)$$

where c and c_0 are constants. As we go back to the past, the amplitude of $\delta R_{\rm osc}$ dominates over $R^{(0)}$, unless the coefficient c is chosen to be very small. Since R gets smaller than R_1 and even becomes negative, the stability condition (4) is

violated. This property also holds in the radiation era during which $\delta R_{\rm osc}$ and the background Ricci scalar $R^{(0)}$ evolve as

$$\delta R_{\rm osc} \simeq c t^{-(9p+15)/8} \cos(c_0 t^{-(1/4)(3p-1)}), \qquad R^{(0)} \propto t^{-3/2}. \tag{48}$$

Thus we need to avoid the excessive production of scalarons in the early universe so that $|\delta R_{\rm osc}| \ll R^{(0)}$ is satisfied at all times. This problem is even severe for the models of the type (21). Moreover, the scalaron mass rapidly grows to the past in these models and can exceed the Planck mass even during the matter era.

The special solution $\delta F_{\rm ind}$ of Eq. (45) can be derived by using the approximation used in Refs. [34,35]. This amounts to neglecting the first and second terms relative to others, giving

$$\delta F_{\rm ind} \simeq f_{,RR} \delta \rho_m, \qquad \delta R_{\rm ind} \simeq \delta \rho_m. \tag{49}$$

Under the condition $|\delta F_{\rm osc}| \ll |\delta F_{\rm ind}|$ we have $\delta F \simeq f_{,RR}\delta\rho_m$. Substituting this relation for Eq. (43) and using the property $M^2 \gg k^2/a^2$, we obtain

$$\ddot{\delta}_m + 2H\dot{\delta}_m - 4\pi G \rho_m \delta_m \simeq 0. \tag{50}$$

Here we have reproduced the gravitational constant for clarity. This is the usual equation of matter perturbations on subhorizon modes in ΛCDM cosmology and has a growing mode solution $\delta_m \propto a \propto t^{2/3}$. From Eq. (49) we get

$$\delta F_{\rm ind} \propto t^{2p+2/3}, \qquad \delta R_{\rm ind} \propto t^{-4/3}. \tag{51}$$

Compared to the oscillating mode (47), the matter-induced mode $\delta R_{\rm ind}$ decreases more slowly and thus dominates in the late universe. Relative to the background value $R^{(0)}$, the perturbation, $\delta R = \delta R_{\rm osc} + \delta R_{\rm ind}$, evolves as

$$\frac{\delta R}{R^{(0)}} \simeq b_1 t^{-(3p+1)/2} \cos(c_0 t^{-p}) + b_2 t^{2/3}, \tag{52}$$

where b_1 and b_2 are constants. Unless the coefficient b_1 is very small, the oscillating mode dominates over the matter-induced mode to violate the condition $R \geq R_1$ as we go back to the past. In Fig. 4 we show an example about the evolution of perturbations in which the initial condition of δR is chosen to be very close to $\delta\rho_m$ (see the appendix for perturbation equations suitable for numerical calculations). The perturbation evolves as $\delta R \propto t^{-4/3}$ during the period in which the condition $M^2 \gg k^2/a^2$ is satisfied. After the system enters the region $M^2 \ll k^2/a^2$, δR decreases more rapidly as we see in the next subsection. Since $\delta R \simeq \delta\rho_m$ and $R^{(0)} \simeq 3H^2 \simeq \rho_m$ during the matter era, we obtain the relation $\delta R/R^{(0)} \simeq \delta_m$. This property is in fact confirmed in Fig. 4 in the region $M^2 \gg k^2/a^2$.

Figure 5 is the case in which the oscillating mode dominates over $\delta R_{\rm ind}$ around the redshift $z \gtrsim 30$. Since $|\delta R|$ grows to the order of $R^{(0)}$ the Ricci scalar R becomes negative in this region, thus violating the stability condition (4). These results confirm that the coefficient b_1 should be chosen to be very small to avoid the dominance of the scalaron mode in an early epoch.

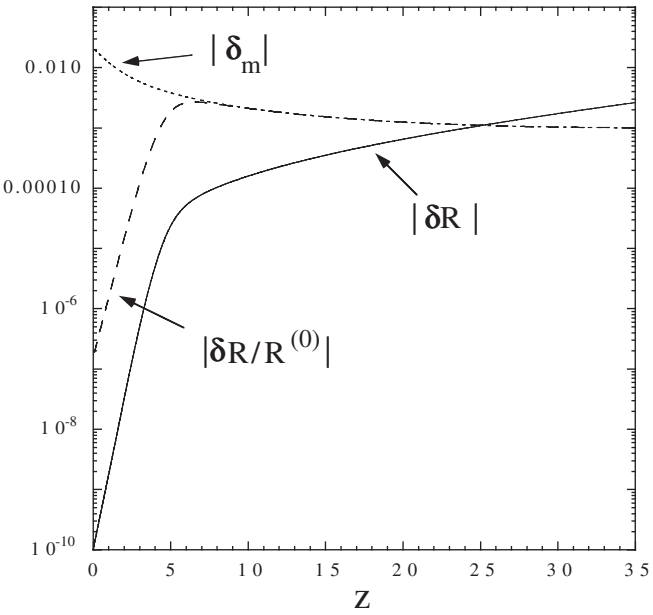

FIG. 4. The evolution of δR, $\delta R/R^{(0)}$, and δ_m for the model $m(r) = (-r-1)^3$ with the mode $k/a_0H_0 = 335$ in the case where the coefficient b_1 in Eq. (52) is very small so that the scalaron mode $\delta R_{\rm osc}$ is negligible relative to the matter-induced mode $\delta R_{\rm ind}$. The transition from the region $M^2 \gg k^2/a^2$ to the region $M^2 \ll k^2/a^2$ occurs around the redshift $z_k = 5$.

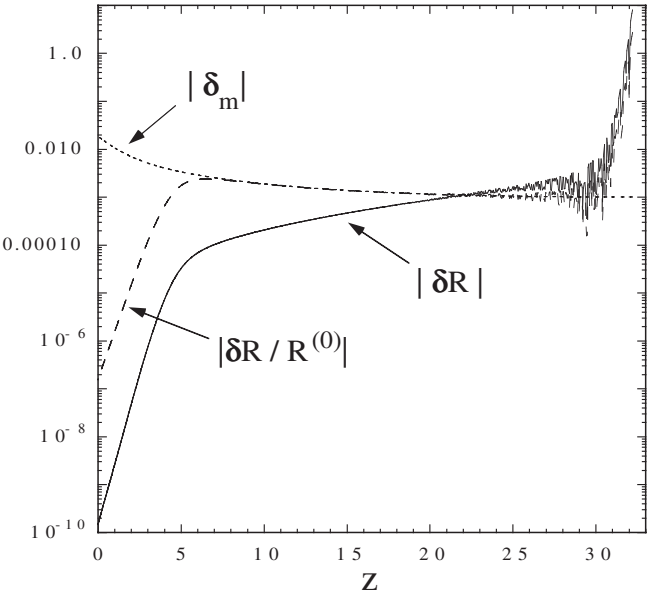

FIG. 5. The evolution of δR, $\delta R/R^{(0)}$, and δ_m for the model $m(r) = (-r-1)^3$ with the mode $k/a_0H_0 = 315$ in the case where the coefficient b_1 in Eq. (52) is not chosen to be very small. The scalaron mode $\delta R_{\rm osc}$ dominates over the matter-induced mode $\delta R_{\rm ind}$ around the redshift $z \gtrsim 30$.

B. The region $M^2 \ll k^2/a^2$

Since the scalaron mass decreases as $M \propto t^{-(p+1)}$, the modes which initially exist in the region $M^2 \gg k^2/a^2$ can enter the regime $M^2 \ll k^2/a^2$ during the matter-dominated epoch. In this regime Eq. (44) is approximately given by

$$\delta\ddot{F} + 3H\delta\dot{F} + \frac{k^2}{a^2}\delta F \simeq \frac{1}{3}\delta\rho_m. \tag{53}$$

Using the WKB approximation, the solution corresponding to the scalaron mode is

$$\delta R_{\rm osc} = \frac{\delta F_{\rm osc}}{f_{,RR}} \simeq ct^{-2p-8/3}\cos(c_0 k t^{1/3}). \tag{54}$$

The matter-induced special solution of Eq. (53) is approximately given by

$$\delta F_{\rm ind} \simeq \frac{a^2}{3k^2}\delta\rho_m. \tag{55}$$

From Eq. (43) we obtain the following approximate equation under the condition $|\delta F_{\rm osc}| \ll |\delta F_{\rm ind}|$:

$$\ddot{\delta}_m + 2H\dot{\delta}_m - \tfrac{4}{3}\cdot 4\pi G\rho_m\delta_m \simeq 0. \tag{56}$$

Relative to the region $M^2 \gg k^2/a^2$ the growth rate of δ_m is enhanced and is given by

$$\delta_m \propto t^{((\sqrt{33}-1)/6)}. \tag{57}$$

Hence the matter-induced mode evolves as

$$\delta F_{\rm ind} \propto t^{(\sqrt{33}-5)/6}, \qquad \delta R_{\rm ind} \propto t^{-2p+(\sqrt{33}-17)/6}. \tag{58}$$

Then the evolution of the perturbation $\delta R = \delta R_{\rm osc} + \delta R_{\rm ind}$, relative to $R^{(0)}$, is given by

$$\frac{\delta R}{R^{(0)}} \simeq b_1 t^{-(2p-2)/3}\cos(c_0 k t^{1/3}) + b_2 t^{-2p+(\sqrt{33}-5)/6}. \tag{59}$$

As long as the scalaron mode is suppressed at the beginning of the matter era, the second term on the r.h.s. of Eq. (59) dominates over the first one. In Figs. 4 and 5 the sudden decrease of δR means that the system enters the region $M^2 \ll k^2/a^2$ in which the evolution of δR is characterized by $\delta R \propto t^{-2p+(\sqrt{33}-17)/6}$. At this stage $\delta R/R^{(0)}$ is no longer proportional to δ_m.

C. The matter power spectra

The evolution of the matter perturbation is given by $\delta_m \propto t^{2/3}$ for $M^2 \gg k^2/a^2$ and $\delta_m \propto t^{(\sqrt{33}-1)/6}$ for $M^2 \ll k^2/a^2$. We shall use the subscript "k" for the quantities at which k is equal to aM, whereas the subscript "Λ" is used at which the accelerated expansion starts ($\ddot{a} = 0$). While the redshift z_Λ is independent of k, z_k depend on k and also on the mass M.

In Table II we show numerical values of z_Λ and z_k for the mode $k/a_0H_0 = 300$ in the model $m(r) = (-r-1)^p$. For smaller p the period of a nonstandard evolution of δ_m becomes longer because z_k tends to be larger. We also note that, for larger k, z_k gets larger. This means that the duration of the period of an additional amplification of δ_m is different depending on the mode k, see Fig. 6. Since the time t_k has a dependence $t_k \propto k^{-3/(3p+1)}$, the matter power spectrum $P_{\delta_m} = (k^3/2\pi^2)|\delta_m|^2$ at the time t_Λ shows a difference compared to the case of the ΛCDM model:

$$\frac{P_{\delta_m}(t_\Lambda)}{P^{\Lambda{\rm CDM}}_{\delta_m}(t_\Lambda)} = \left(\frac{t_\Lambda}{t_k}\right)^{2(((\sqrt{33}-1)/6)-(2/3))} \propto k^{(\sqrt{33}-5)/(3p+1)}. \tag{60}$$

While the galaxy matter power spectrum is modified by this effect, the CMB spectrum is hardly affected except for

TABLE II. The redshifts z_Λ and z_k in the model $m(r) = (-r-1)^p$ for the mode $k/a_0H_0 = 300$. We also show analytic and numerical values of $\delta n(t_\Lambda)$, which are denoted as $\delta n^{(\rm A)}(t_\Lambda)$ and $\delta n^{(\rm N)}(t_\Lambda)$, respectively. The values $\delta n^{(\rm N)}(t_0)$ are obtained by numerically integrating perturbation equations up to the present epoch.

p	z_Λ	z_k	$\delta n^{(\rm A)}(t_\Lambda)$	$\delta n^{(\rm N)}(t_\Lambda)$	$\delta n^{(\rm N)}(t_0)$
2	0.95	9.62	0.106	0.107	0.108
3	0.86	4.83	0.075	0.074	0.077
4	0.81	3.25	0.057	0.056	0.061
5	0.78	2.49	0.047	0.045	0.053
6	0.76	2.03	0.039	0.035	0.044
7	0.75	1.72	0.034	0.028	0.039

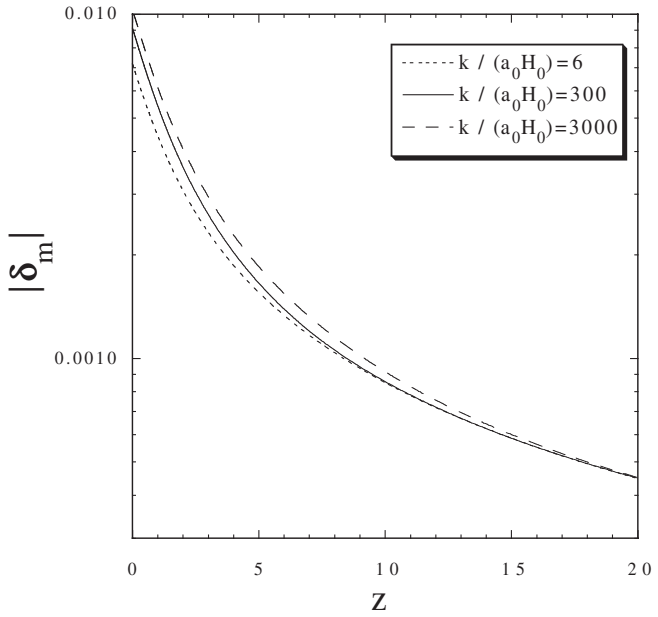

FIG. 6. The evolution of the matter perturbation δ_m in the model $m(r) = (-r-1)^2$ for the modes $k/a_0H_0 = 6$, 300, 3000. The transition redshift z_k increases for larger k. For the mode $k/a_0H_0 = 300$ we have $z_k = 9.62$.

low multipoles around which an integrated Sachs-Wolfe (ISW) effect becomes important [36]. Thus there is a difference for the spectral indices of two power spectra, i.e.,

$$\delta n(t_\Lambda) = \frac{\sqrt{33} - 5}{3p + 1}. \tag{61}$$

Since z_k becomes as close as z_Λ for larger p, it is not necessarily guaranteed that Eq. (61) is valid in such cases. Moreover the estimation (61) does not take into account the evolution of δ_m after $z = z_\Lambda$ to the present epoch ($z = 0$). In order to see the validity of the formula (61) we have evaluated numerical values of $\delta n(t_\Lambda)$ as well as $\delta n(t_0)$ integrated up to the present epoch. From Table II we find that the estimation (61) agrees well with the numerically obtained $\delta n(t_\Lambda)$ for $p \leq 5$. The difference appears for $p \geq 6$, but it is not significant.

After the system enters the epoch of an accelerated expansion, the momentum k can again become smaller than aM. Hence the k-dependence is not necessarily negligible even for $z < z_\Lambda$. However we find from Table II that $\delta n(t_0)$ is not much different from $\delta n(t_\Lambda)$ derived by Eq. (61). Thus the analytic estimation (61) is certainly reliable to place constraints on model parameters except for $p \gg 1$.

Observationally we do not find any strong signature for the difference of slopes of the spectra of LSS and CMB [37]. If we take the mild bound $\delta n \lesssim 0.05$, we obtain the constraint $p \geq 5$. It is interesting to recall that LGC are well satisfied for $p \geq 5$.

Finally we shall discuss the integrated Sachs-Wolfe (ISW) effect in the model $m(r) = C(-r - 1)^p$. In order to confront the model with CMB it is convenient to study the evolution of an effective gravitational potential $\Phi \equiv (\alpha - \varphi)/2$ in the longitudinal gauge ($\chi = 0$) [20,33]. Under the subhorizon approximation used in Refs. [34,35] we obtain, from Eqs. (41) and (42), the following relation

$$\Phi \simeq -\frac{3}{2}\frac{a^2H^2}{k^2}\Omega_m\delta_m. \tag{62}$$

In the ΛCDM model the gravitational potential remains constant during the standard matter era, but it decays after the system enters the accelerated epoch. This leads to the ISW effect for low multipoles of the CMB power spectrum. In our $f(R)$ model (16), the additional growth of matter perturbations in the region $z < z_k$ changes the evolution of Φ.

In Fig. 7 we plot the evolution of Φ in the models $m(r) = (-r - 1)^p$ with the mode $k/a_0H_0 = 4$ for several different values of p. For smaller p the gravitational potential does not decay much because the duration of the region $z < z_k$ gets longer. The models that cancel the ISW effect by the additional growth of δ_m are consistent with the CMB data [36], which means that the models with $p \geq 2$ are allowed. Hence the information coming from the ISW effect of CMB does not provide strong constraints on the model parameters compared to the galaxy spectrum discussed above.

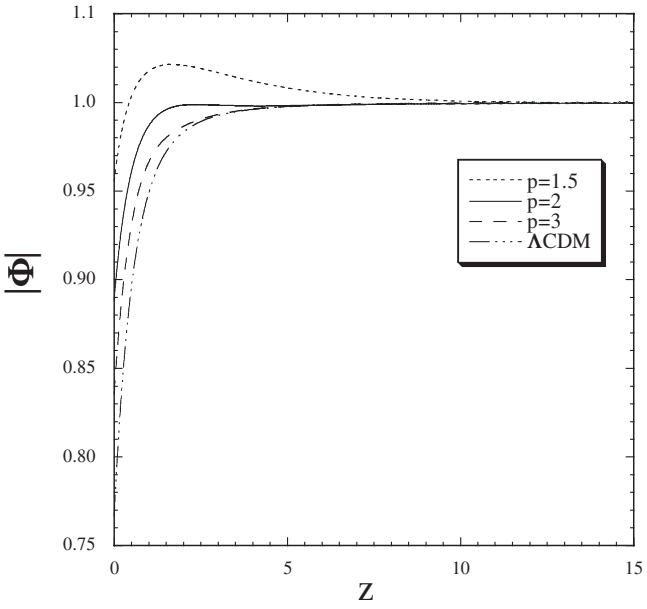

FIG. 7. The evolution of the effective gravitational potential $\Phi \equiv (\alpha - \varphi)/2$ in the model $m(r) = (-r - 1)^p$ for the mode $k/a_0H_0 = 4$ with three different values of p. Note that Φ is initially normalized as unity. We also show the evolution of Φ in the ΛCDM model. For larger p the decay of the gravitational potential is more significant. When $p \geq 2$ the models are well consistent with CMB low multipole data.

V. CONCLUSIONS

We have discussed various observational signatures of $f(R)$ dark energy scenarios that satisfy both cosmological and local gravity constraints. The $f(R)$ models do not have much freedom to fulfill all such constraints. Generally the models need to mimic the ΛCDM model in a high-curvature region where local gravity experiments are carried out ($R \gg R_0 \sim H_0^2$). The deviation from the ΛCDM cosmology becomes important after the end of the matter-dominated epoch in such viable models.

The models given in Eqs. (11) and (12) belong to such viable classes that possess a de-Sitter attractor at $R = R_1 > 0$ and satisfy the condition $f(R = 0) = 0$. The stability conditions require that $f_{,R} > 0$ and $f_{,RR} > 0$ for $R \geq R_1$. In the models (11) and (12) either of these stability conditions is violated in the region $R < R_1$, but this is not problematic as long as the Ricci scalar does not oscillate. In Sec. II we discussed general properties about viable $f(R)$ models and proposed another simple model (21) that can satisfy the conditions $f_{,R} > 0$ and $f_{,RR} > 0$ for all positive R.

The model we have studied in this paper is given by $m(r) = C(-r - 1)^p$ ($C > 0$, $p > 1$), where m and r are

defined by Eq. (3). In the high-curvature region characterized by $R \gg R_0$, this recovers the models (11) and (12) with finite p and also the model (21) with $p \to \infty$. Moreover the departure from the ΛCDM cosmology can be captured by the growth of the quantity m as the solutions approach the de-Sitter fixed point on the line $r = -2$. In fact this model possesses rich observational signatures relevant to SN Ia, galaxy clustering, and CMB.

The equation of state of dark energy shows a peculiar divergent behavior with a cosmological boundary crossing. When the deviation from the ΛCDM model is significant, the redshift z_c at which such a divergence occurs can be as close as a few. This may be detectable in future observations of SN Ia and weak lensing. Using observational bounds on the equation of state of dark energy at present ($z = 0$), we found that the models with $p \geq 2$ are consistent with the data. The deviation parameter m is constrained to be $m(z = 0) \lesssim 0.3$. We also showed that the models with $p \geq 2$ satisfy sound horizon constraints of the CMB.

We have discussed the evolution of matter density perturbations δ_m together with the perturbation in the Ricci scalar R. The mass squared of the scalaron, $M^2 \simeq 1/(3f_{,RR})$, is much larger than H^2 and can cross the value k^2/a^2 during the matter era. In the early epoch with $M^2 \gg k^2/a^2$ the matter perturbation evolves as in the standard way, provided that the oscillating mode $\delta R_{\rm osc}$ (scalaron) is suppressed relative to the matter-induced mode $\delta R_{\rm ind}$. However the scalaron dominates at early epochs unless the coefficient of this mode is chosen to be very small so that δR is always as close as $\delta R_{\rm ind}$. The dominance of the scalaron means the violation of the condition (4), which leads to an instability of solutions in the matter-dominated epoch. This property persists in the radiation era and hence it poses a problem about how an overproduction of the scalaron is avoided in the early universe.

In the late epoch characterized by $M^2 \ll k^2/a^2$ the matter perturbation evolves in a nonstandard way, see Eq. (56). This leads to additional growth of matter perturbations depending on the wave number k. Considering the evolution of δ_m by the time t_Λ at which an accelerated expansion sets in, the difference about spectral indices of the power spectra between galaxy clustering and CMB is given by Eq. (61). We also integrated perturbation equations numerically by the present epoch and found that the estimation (61) agrees fairly well with numerical values. Using the rather mild criterion $\delta n \lesssim 0.05$, the constraint on the parameter p is given by $p \geq 5$. We have also studied the evolution of an effective gravitational potential and found that the integrated Sachs-Wolfe effect in low multipoles of the CMB does not provide a stronger constraint than the one coming from LSS.

It will be certainly of interest to place stringent constraints on the model parameters using future high-precision observational data. We hope that this allows us to find some signatures about the deviation from the ΛCDM model. In particular the detection of unusual behavior of the equation of state of dark energy can be strong evidence for $f(R)$ gravity models.

ACKNOWLEDGMENTS

I thank Luca Amendola, Nicola Bartolo, Daniel Bertacca, Antonio De Felice, Martin Kunz, Sabino Matarrese, David Polarski, Alexei Starobinsky, Reza Tavakol, and Kotub Uddin for very useful discussions. I am also grateful to Roy Maartens, Reza Tavakol, Luca Amendola, and Sabino Matarrese for supporting visits to University of Portsmouth, University of Queen Mary, Rome observatory, and University of Padova during which this work was completed.

APPENDIX

In this appendix we present the perturbation equations convenient for numerical purposes. We neglect the contribution of radiation, i.e., $x_4 = 0$. Using the dimensionless variables given in Eq. (27) and introducing a new quantity $\delta\tilde{F} = \delta F/F$, Eqs. (43) and (44) can be written as

$$\delta_m'' + \left(x_3 - \frac{1}{2}x_1\right)\delta_m' - \frac{3}{2}(1 - x_1 - x_2 - x_3)\delta_m = \frac{1}{2}\left[\left\{\frac{k^2}{x_5^2} - 6 + 3x_1^2 - 3x_1' - 3x_1(x_3 - 1)\right\}\delta\tilde{F} + 3(-2x_1 + x_3 - 1)\delta\tilde{F}' + 3\delta\tilde{F}''\right], \tag{A1}$$

$$\delta\tilde{F}'' + (1 - 2x_1 + x_3)\delta\tilde{F}' + \left[\frac{k^2}{x_5^2} - 2x_3 + \frac{2x_3}{m} - x_1(x_3 + 1) - x_1' + x_1^2\right]\delta\tilde{F} = (1 - x_1 - x_2 - x_3)\delta_m - x_1\delta_m', \tag{A2}$$

where a new variable, $x_5 \equiv aH$, satisfies

$$x_5' = (x_3 - 1)x_5. \tag{A3}$$

Note that the perturbation δR is given by

$$\delta R = 6H^2\frac{x_3}{m}\delta\tilde{F}. \tag{A4}$$

The evolution of the Hubble parameter is known by solving the equation

$$\frac{H'}{H} = x_3 - 2. \tag{A5}$$

Solving Eqs. (A1) and (A2) together with the background equations (28)–(30), (A3), and (A5), numerically, we find the evolution of δ_m and δR.

[1] V. Sahni and A. A. Starobinsky, Int. J. Mod. Phys. D **9**, 373 (2000); S. M. Carroll, Living Rev. Relativity **4**, 1 (2001); V. Sahni, Lect. Notes Phys. **653**, 141 (2004); T. Padmanabhan, Phys. Rep. **380**, 235 (2003); P. J. E. Peebles and B. Ratra, Rev. Mod. Phys. **75**, 559 (2003); S. Nojiri and S. D. Odintsov, Int. J. Geom. Methods Mod. Phys. **4**, 115 (2007).

[2] E. J. Copeland, M. Sami, and S. Tsujikawa, Int. J. Mod. Phys. D **15**, 1753 (2006).

[3] A. A. Starobinsky, Phys. Lett. B **91B**, 99 (1980).

[4] S. Capozziello, V. F. Cardone, S. Carloni, and A. Troisi, Int. J. Mod. Phys. D **12**, 1969 (2003); S. Capozziello, S. Carloni, and A. Troisi, arXiv:astro-ph/0303041; S. M. Carroll, V. Duvvuri, M. Trodden, and M. S. Turner, Phys. Rev. D **70**, 043528 (2004).

[5] S. Capozziello, F. Occhionero, and L. Amendola, Int. J. Mod. Phys. D **1**, 615 (1992).

[6] S. Nojiri and S. D. Odintsov, Phys. Rev. D **68**, 123512 (2003); M. E. Soussa and R. P. Woodard, Gen. Relativ. Gravit. **36**, 855 (2004); G. Allemandi, A. Borowiec, and M. Francaviglia, Phys. Rev. D **70**, 103503 (2004); D. A. Easson, Int. J. Mod. Phys. A **19**, 5343 (2004); S. M. Carroll *et al.*, Phys. Rev. D **71**, 063513 (2005); S. Carloni, P. K. S. Dunsby, S. Capozziello, and A. Troisi, Classical Quantum Gravity **22**, 4839 (2005).

[7] A. D. Dolgov and M. Kawasaki, Phys. Lett. B **573**, 1 (2003).

[8] T. Chiba, Phys. Lett. B **575**, 1 (2003).

[9] L. Amendola, D. Polarski, and S. Tsujikawa, Phys. Rev. Lett. **98**, 131302 (2007); arXiv:astro-ph/0605384.

[10] S. Capozziello, S. Nojiri, S. D. Odintsov, and A. Troisi, Phys. Lett. B **639**, 135 (2006); A. W. Brookfield, C. van de Bruck, and L. M. H. Hall, Phys. Rev. D **74**, 064028 (2006); M. Amarzguioui, O. Elgaroy, D. F. Mota, and T. Multamaki, Astron. Astrophys. **454**, 707 (2006); T. P. Sotiriou, Classical Quantum Gravity **23**, 5117 (2006); S. Nojiri and S. D. Odintsov, Phys. Rev. D **74**, 086005 (2006); N. J. Poplawski, Phys. Rev. D **74**, 084032 (2006); A. Borowiec, W. Godlowski, and M. Szydlowski, Phys. Rev. D **74**, 043502 (2006); T. Koivisto, Phys. Rev. D **73**, 083517 (2006); A. de la Cruz-Dombriz and A. Dobado, Phys. Rev. D **74**, 087501 (2006); T. Multamaki and I. Vilja, Phys. Rev. D **74**, 064022 (2006); T. P. Sotiriou, Phys. Lett. B **645**, 389 (2007); T. P. Sotiriou and S. Liberati, Ann. Phys. (N.Y.) **322**, 935 (2007); V. Faraoni and S. Nadeau, Phys. Rev. D **75**, 023501 (2007); D. Huterer and E. V. Linder, Phys. Rev. D **75**, 023519 (2007); S. Fay, R. Tavakol, and S. Tsujikawa, Phys. Rev. D **75**, 063509 (2007); K. Kainulainen, J. Piilonen, V. Reijonen, and D. Sunhede, Phys. Rev. D **76**, 024020 (2007); A. De Felice and M. Hindmarsh, J. Cosmol. Astropart. Phys. 06 (2007) 028; K. Uddin, J. E. Lidsey, and R. Tavakol, Classical Quantum Gravity **24**, 3951 (2007); J. C. C. de Souza and V. Faraoni, Classical Quantum Gravity **24**, 3637 (2007); M. S. Movahed, S. Baghram, and S. Rahvar, Phys. Rev. D **76**, 044008 (2007); E. O. Kahya and V. K. Onemli, arXiv:gr-qc/0612026; M. Fairbairn and S. Rydbeck, arXiv:astro-ph/0701900; P. J. Zhang, Phys. Rev. D **73**, 123504 (2006); Phys. Rev. D **76**, 024007 (2007); G. Cognola, M. Gastaldi, and S. Zerbini, arXiv:gr-qc/0701138; D. Bazeia, B. Carneiro da Cunha, R. Menezes, and A. Y. Petrov, arXiv:hep-th/0701106; T. Rador, Phys. Rev. D **75**, 064033 (2007); S. Bludman, arXiv:astro-ph/0702085; L. M. Sokolowski, arXiv:gr-qc/0702097; S. Fay, S. Nesseris, and L. Perivolaropoulos, Phys. Rev. D **76**, 063504 (2007); S. Nojiri, S. D. Odintsov, and P. V. Tretyakov, Phys. Lett. B **651**, 224 (2007); O. Bertolami, C. G. Boehmer, T. Harko, and F. S. N. Lobo, Phys. Rev. D **75**, 104016 (2007); S. Capozziello and M. Francaviglia, arXiv:0706.1146; A. De Felice, P. Mukherjee, and Y. Wang, arXiv:0706.1197; B. Li, J. D. Barrow, and D. F. Mota, Phys. Rev. D **76**, 104047 (2007); K. Bamba, Z. K. Guo, and N. Ohta, arXiv:0707.4334; C. G. Boehmer, T. Harko, and F. Lobo, arXiv:0709.0046; C. G. Boehmer, T. Harko, and F. S. N. Lobo, arXiv:0709.0046.

[11] L. Amendola, R. Gannouji, D. Polarski, and S. Tsujikawa, Phys. Rev. D **75**, 083504 (2007).

[12] B. Li and J. D. Barrow, Phys. Rev. D **75**, 084010 (2007).

[13] L. Amendola and S. Tsujikawa, arXiv:0705.0396.

[14] W. Hu and I. Sawicki, Phys. Rev. D **76**, 064004 (2007).

[15] A. A. Starobinsky, JETP Lett. **86**, 157 (2007).

[16] S. A. Appleby and R. A. Battye, Phys. Lett. B **654**, 7 (2007).

[17] G. J. Olmo, Phys. Rev. D **72**, 083505 (2005).

[18] G. J. Olmo, Phys. Rev. Lett. **95**, 261102 (2005); A. L. Erickcek, T. L. Smith, and M. Kamionkowski, Phys. Rev. D **74**, 121501 (2006); V. Faraoni, Phys. Rev. D **74**, 023529 (2006); A. F. Zakharov, A. A. Nucita, F. De Paolis, and G. Ingrosso, Phys. Rev. D **74**, 107101 (2006); I. Navarro and K. Van Acoleyen, J. Cosmol. Astropart. Phys. 02 (2007) 022; T. Chiba, T. L. Smith, and A. L. Erickcek, Phys. Rev. D **75**, 124014 (2007); G. Allemandi and M. L. Ruggiero, Gen. Relativ. Gravit. **39**, 1381 (2007); X. H. Jin, D. J. Liu, and X. Z. Li, arXiv:astro-ph/0610854; T. Faulkner, M. Tegmark, E. F. Bunn, and Y. Mao, Phys. Rev. D **76**, 063505 (2007); S. Nojiri and S. D. Odintsov, arXiv:0707.1941.

[19] V. Faraoni, Phys. Rev. D **74**, 104017 (2006).

[20] Y. S. Song, W. Hu, and I. Sawicki, Phys. Rev. D **75**, 044004 (2007); I. Sawicki and W. Hu, Phys. Rev. D **75**, 127502 (2007).

[21] N. Agarwal and R. Bean, arXiv:0708.3967.

[22] J. Khoury and A. Weltman, Phys. Rev. Lett. **93**, 171104 (2004); Phys. Rev. D **69**, 044026 (2004).

[23] S. Tsujikawa, K. Uddin, and R. Tavakol, arXiv:0712.0082; S. Capozziello and S. Tsujikawa, arXiv:0712.2268.

[24] C. D. Hoyle, D. J. Kapner, B. R. Heckel, E. G. Adelberger, J. H. Gundlach, U. Schmidt, and H. E. Swanson, Phys. Rev. D **70**, 042004 (2004).

[25] I. I. Shapiro, Phys. Rev. Lett. **13**, 789 (1964).

[26] S. Nesseris and L. Perivolaropoulos, J. Cosmol. Astropart. Phys. 01 (2007) 018; Phys. Rev. D **75**, 023517 (2007).

[27] P. Astier *et al.*, Astron. Astrophys. **447**, 31 (2006).

[28] A. Shafieloo, U. Alam, V. Sahni, and A. A. Starobinsky, Mon. Not. R. Astron. Soc. **366**, 1081 (2006); A. Shafieloo, arXiv:astro-ph/0703034.

[29] D. N. Spergel *et al.*, Astrophys. J. Suppl. Ser. **170**, 377 (2007).

[30] L. Amendola, Phys. Rev. D **62**, 043511 (2000).

[31] H. Kodama and M. Sasaki, Prog. Theor. Phys. Suppl. **78**, 1 (1984); V. F. Mukhanov, H. A. Feldman, and R. H.

Brandenberger, Phys. Rep. **215**, 203 (1992); B. A. Bassett, S. Tsujikawa, and D. Wands, Rev. Mod. Phys. **78**, 537 (2006).

[32] J. c. Hwang and H. Noh, Phys. Rev. D **71**, 063536 (2005); Phys. Rev. D **66**, 084009 (2002).

[33] S. M. Carroll, I. Sawicki, A. Silvestri, and M. Trodden, New J. Phys. **8**, 323 (2006); R. Bean, D. Bernat, L. Pogosian, A. Silvestri, and M. Trodden, Phys. Rev. D **75**, 064020 (2007); L. Pogosian and A. Silvestri, Phys. Rev. D **77**, 023503 (2008); I. Laszlo and R. Bean, arXiv:0709.0307.

[34] B. Boisseau, G. Esposito-Farese, D. Polarski, and A. A. Starobinsky, Phys. Rev. Lett. **85**, 2236 (2000); G. Esposito-Farese and D. Polarski, Phys. Rev. D **63**, 063504 (2001).

[35] S. Tsujikawa, Phys. Rev. D **76**, 023514 (2007).

[36] Y. S. Song, H. Peiris, and W. Hu, Phys. Rev. D **76**, 063517 (2007).

[37] M. Tegmark *et al.*, Phys. Rev. D **74**, 123507 (2006).